

Available online at www.sciencedirect.com**Physics
Procedia**

Physics Procedia 5 (2010) 495–502

www.elsevier.com/locate/procedia

LANE 2010

Defect formation in glass welding by means of ultra short laser pulses

Kristian Cvecek^{a,*}, Ilya Alexeev^b, Isamu Miyamoto^c, Michael Schmidt^{a,b}^a*Bayerisches Laserzentrum GmbH, Konrad-Zuse-Str. 2-6, 91052 Erlangen, Germany*^b*Lehrstuhl für Photonische Technologien, Paul-Gordan-Str. 3, 91052 Erlangen, Germany*^c*1-12, Koshien 4-Bancho, Nishinomiya, 663-8174 Hyogo, Japan*

Abstract

Many applications require a joining of several glass components. However, the established processes for glass joining have certain disadvantages. By contrast, laser fusion welding by ultrafast lasers exhibits in principle excellent versatility, if the nonlinear interaction is localized enough so that plasma induced stresses can be tolerated and the temperature is high enough to melt the glass adjacent to the focal spot. However, defect generation during welding was observed for a broad range of welding conditions. This paper reports the observed defects and analyzes their origins.

© 2010 Published by Elsevier B.V. Open access under [CC BY-NC-ND license](https://creativecommons.org/licenses/by-nc-nd/4.0/).

Keywords: laser materials processing; glass and other amorphous materials; ultrafast lasers, welding; glass welding

1. Introduction

Glass is a widely used material in many applications such as optics, telecommunications, electronics, MEMS, biomedicine, as well as construction industry and design because of its excellent physical and chemical properties. Many of these applications require an assembly or joining of two or more glass parts. For the task of joining several different technologies have been developed, each with specific properties that make it useful only within a limited application range.

The major disadvantage of, e.g. a mechanical assembly of glass is a mismatch between the thermal expansion coefficients of glass and the mount material because of the high sensitivity of glass towards tensile and compressive stresses especially under alternating thermal and/or vibrational loads [1]. Moreover, the mechanical mounting technology can be miniaturized only within certain limits imposed by the manufacturability of the mechanical components.

Also other joining technologies such as gluing and soldering suffer from a mismatch between the thermal expansion coefficients of glass and the adhesive or solder. UV-curable glues are often hazardous to health and

* Corresponding author. Tel.: +49-9131-9779037; fax: +49-9131-9779011.

E-mail address: k.cvecek@blz.org.

undergo a shrinkage process that leads to inherent stresses at the joining surface. The organic structure of the adhesive limits the maximum optical power that can be transmitted through the glued components. Moreover, the long term stability of the joint can be reduced in damp and chemically aggressive environs [2]. To some extent soldering is a similar method to gluing and therefore typically suffers from similar issues such as inherent mechanical stresses as well as from a reduced durability in chemically aggressive environs and a reduced optical damage threshold.

Optical contacting is used to join optical components without any joining additives [3]. This is accomplished by using components where the conjugate facets have the same curvature, a sufficiently small surface roughness, and which are thoroughly cleaned. Then, if brought into close proximity, the components are bound together by Van-der-Waals-interactions. The primary disadvantage of this method is that the optical contact is highly susceptible to impact loads [4].

In solid-state diffusion bonding, optically contacted glass plates are heated to high temperature, while high pressure is applied. Under these conditions local plastic deformations occur that enhance inter-diffusion at the joining surface. The bonding joint consists of the base materials and has therefore almost the same resistance against aggressive chemical environs or alternating thermal loads as the base material itself [5]. However, the diffusion bonding requires relatively long time because the joining process depends on atomic diffusion. The bonding process is also limited to certain geometries of the components, e. g. plates, since the glass components have to withstand high pressure and temperature during the process.

Laser fusion welding by linear absorption without a pre- and post-heating procedure has been successfully demonstrated so far only for fused silica using a CW CO₂-laser [6]. Other glass types have a significantly larger thermal expansion coefficient which leads to the development of cracks during the cooling period, because of the brittleness of glass. Cracking can be prevented by pre- and post- heating to provide ductility to the glass [7]. In that case, the achieved mechanical strength of joint seams can be as high as that of the base material. However, pre- and post- heating can be problematic for scientific and industrial applications due to an increased process complexity, a reduced throughput, and an incompatibility of materials with different thermal durability. Moreover, welding based on linear absorption cannot be carried out with readily available solid state lasers without using an absorber material as glasses are typically transparent for this wavelength range.

The need for a far infrared laser or an absorbent can be circumvented in the case of ultrashort pulsed laser fusion welding based on nonlinear absorption processes. In this method ultra-short laser pulses, at a wavelength transparent to the processing material, are tightly focused onto the joint surface of two glass pieces intended for welding. Due to the tight focusing and short laser pulse duration, the light intensity inside the focal volume reaches values at which multi-photon ionization can occur. The density of free electrons grows very rapidly, until (after roughly 50-100 fs) [8] it becomes high enough that subsequently avalanche ionization occurs by which the plasma density further significantly increases. As the electron mobility is much higher than the mobility of the crystal lattice it takes around 30 ps until a thermal equilibrium between electrons and ions is reached via electron phonon coupling [9]. In this way hot plasma is generated which is able to heat the surrounding material. In order to reach the melting point it is necessary to have the heating rate higher than the cooling rate. Because the plasma generation takes place only within a very small focal region the cooling time is very short, typically on the order of 10 μ s or less. Therefore, ultrafast glass welding normally requires employment of high repetition rate (on the order of 1 MHz) laser systems.

Because of the highly localized heat generation it is in principle possible to reduce the shrinkage stress during the cooling of the molten zone well below the critical breaking strength of the glass, effectively suppressing the development of thermally induced cracks as has been shown in [10]. However, as will be shown in the present work, crack development is observed for a broad range of conditions in glass welding by ultrafast lasers. The suppression of cracks is an exceedingly important task because an existing crack can have tips that reach into the bulk material at which nearly singular stress fields occur if an outer mechanical load is applied and by which further crack development can be enabled. In order to obtain understanding of the underlying processes which lead to crack development the present work gives an overview on the observed defects while the origins of the most prominent defect types are analyzed and possible solutions for their suppression or prevention are presented.

2. Experimental setup

The schematic of the experimental setup used for glass welding by ultrafast lasers is shown in fig. 1. The laser is a modelocked Nd:YVO₄ laser which generates pulses with a FWHM duration of ca. 10 ps at a wavelength of 1064 nm and with a pulse repetition rate that can be set from 50 kHz up to 8.2 MHz (Duetto, TBWP, Switzerland). The maximum achievable average laser power on a glass sample is 7 W and it can be adjusted by the $\lambda/2$ -waveplate in front of the polarizing beam splitter. The laser beam is focused by specialized near infrared microscope objectives (Olympus), with numerical apertures ranging from 0.4 up to 1.2 (water immersion) into glass samples. Typical focal spot sizes lie between 2 – 6 μm . The beam focus height is adjusted by a manual z-translation stage (not shown) on which the focusing objective lens is mounted. The glass sample is positioned on a motorized x-y translation stage which can achieve translation speeds of up to 300 mm/s.

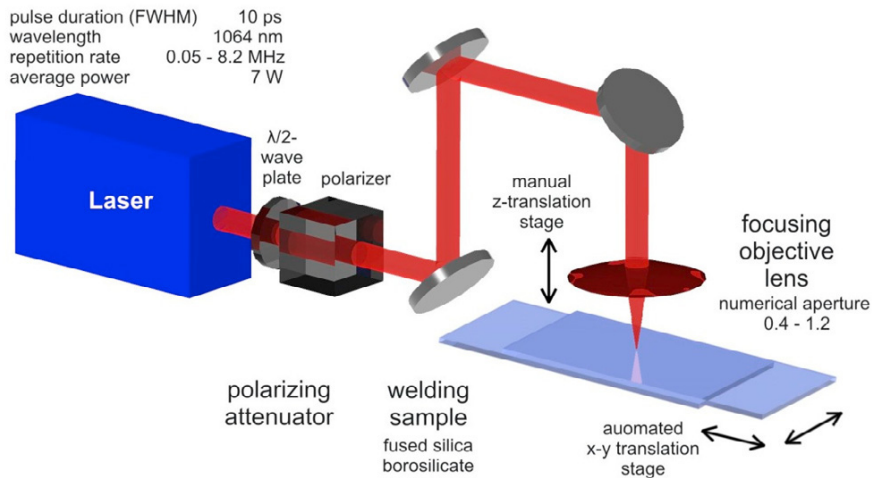


Fig. 1. Schematic of the experimental setup

Prior to laser processing, optical contact is established between the glass samples as described in [10]. The optical contact is strong enough to keep the samples joined if no undue forces act upon them. The glass samples are aligned perpendicularly to the laser beam with an accuracy of $\pm 0.03^\circ$. The focal spot of the laser is set into the vicinity of the joining surface, by first finding the rear side of the upper plate and then moving the focal spot horizontally to the position where the welding shall be performed. As a last step the focal depth must be corrected according to the welding parameters such as average power, repetition rate and welding speed that will be used for welding because the shape and position of the cross section of the welding seam strongly depends on the welding parameters [11]. The procedure for aligning the focal spot with the joining interface is described in greater detail in [10].

Once the welding parameters are set, the x-y translation stage is accelerated. After the feed speed reaches the specified value the laser is triggered on. During the irradiation the feed rate is kept constant. Before the sample decelerates the laser is triggered off.

During the experiments glasses such as fused silica, borosilicate glasses (D263) and fortran have been used that have different thermo-mechanical properties.

3. Experimental results and discussion

During the experiments several types of defects were observed. Some types were common to all examined glass types, others occurred only in specific glass types.

Fig. 2 shows crack formations that were observed in all investigated types of glass. While the actual size and shape of the cracks can vary depending on the glass type and the processing parameters, they all exhibit similar characteristic behaviour. The most apparent common features are the longitudinal orientation of the cracks along the laser beam path and a more pronounced defect formation at the bottom of the molten zone rather than at the top.

We attribute these defects to high internal pressure (that can be a combination of multiple factors) that develops due to the plasma build-up inside the material. At comparably low pulse repetition rates or high feed rates the internal pressure of a plasma region with a high height to width ratio acts against cold and brittle material leading to the formation of cracks. An indicator for the comparably cold material are the gas bubbles trapped along the entire length of the molten zone observed in fused silica glass (fig. 2 (b)) while the spatial distribution bubbles signifies the extents of the plasma shape [10]. The trapping of the gas bubbles happens because the buoyant force experienced by a gas bubble generated inside the plasma is not large enough to overcome the quickly increasing viscosity of the melted glass due to the fast cooling rate. This effect is not observed for larger molten regions.

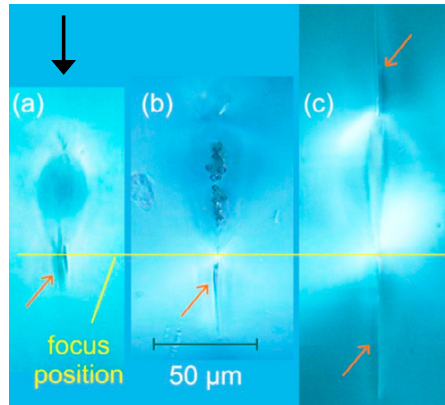


Fig. 2. Sample cross sections of melt run experiments carried out in different glass materials. Cracks, identified by the red arrows, are generated under following conditions: (a): D263, NA = 0.4, P = 2.28 W, $v = 200$ mm/s, $f = 1$ MHz; (b): fudes silica, NA = 0.8, P = 5.6 W, $v = 200$ mm/s, $f = 0.3$ MHz; (c): foturan, NA = 0.55, P = 6 W, $v = 200$ mm/s, $f = 1$ MHz. The laser beam propagation direction is indicated by the black arrow

The length asymmetry of the cracks above and below the molten zone can be ascribed to a nonuniform laser absorption along the beam propagation path as described in [10,11]. These publications have shown that the upper part of the focal volume is heated stronger than the material at the lower part resulting in a teardrop shaped molten zone. Due to the thicker upper part of the molten zone, the material stays viscous longer at the top, whereas the material at the bottom solidifies much faster. Therefore, longitudinal cracks generated above the focal spot can be closed up more easily by the molten zone than cracks below the focal spot, partially decreasing the size of the upper cracks. At the relatively fast feed speed ($v = 200$ mm/s for shown experimental data) the formed molten zone is overall quite small when compared to molten zones shown in fig. 4 and 6. Due to the reduced size of the molten zone the cool-down is much faster which effectively “freezes” the defects within the interaction region especially at its bottom part.

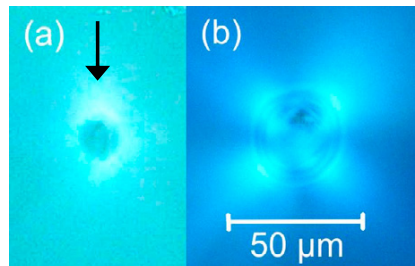


Fig. 3. Cross sections of melt runs carried out at high numerical apertures in D263 and fused silica. The experimental conditions are as follows: (a): D263, NA = 0.8, P = 0.65 W, $v = 200$ mm/s, $f = 1$ MHz; (b): Fused silica, NA = 1.2 (water immersion), P = 9 W (measured in front of the lens), $v = 100$ mm/s, $f = 100$ kHz. The laser beam propagation direction is indicated by the black arrow

The high aspect ratio of the plasma plume inside the focal spot is responsible for the longitudinal cracks shown in fig. 2. The origin of the high height to width ratio lies in the still relatively long Rayleigh length of the laser beam inside the glass material of $18\ \mu\text{m}$ at the numerical aperture of 0.55 used in the experiment. To realize a point-shaped plasma plume with a laser beam, intensity of the beam has to decrease very rapidly along the beam axis outside the laser focus. This can be approximately achieved with focusing lenses that have a numerical aperture (NA) of 0.8 or higher.

Using lenses with high numerical apertures crack free molten zones were achieved at high feed rates in D263 glass (NA=0.8) and fused silica glass (NA=1.2). The results are shown in fig. 3. As can be seen, the molten zones are almost radially symmetric and defect free. The melt run in fig. 3 (a) has an aspect ratio (height/width) of 1.16 while the melt run in fused silica has an aspect ratio of 1.11. A radially symmetric molten zone has a further advantage insofar that any stress field generated during the heating and cooling of glass material is more evenly distributed than in the case of a tear drop shaped molten zone.

While this approach to suppress the formation of longitudinal cracks appears to be quite promising it has to be verified further experimentally and numerically for a much broader set of processing conditions and for the actual glass welding process. However, an issue that has to be taken into account is that using focusing objectives with high numerical apertures spherical waveforms are generated that propagate from a large solid angle. At a plane surface of a material with higher refractive index such as glass these waves are refracted so that beams far from the axis get focused further away than beams near the axis causing a so-called spherical aberration distortion [12]. This aberration increases with growing focusing depth and leads to an elongation of the focal spot and thus back to a nonuniform temperature distribution. In practice, spherical aberrations can be minimized either by focusing the laser beam near the top surface as is the case in fig. 3, by using focusing lens with the possibility to correct for these aberrations or by using an immersion fluid that has a refractive index which is matched to the glass material and the objective lens.

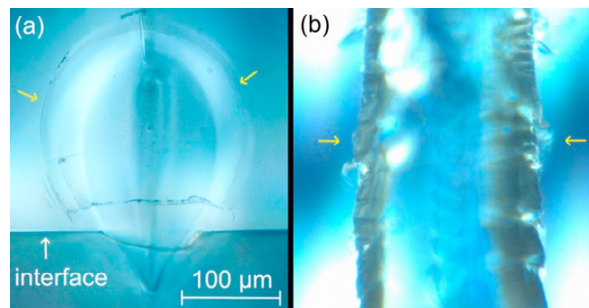


Fig. 4. Cross section (a) and top view (b) of a welding seam in D263 glass. The cracks indicated by the yellow arrows have developed around the molten zone. The welding conditions are: NA = 0.55, P = 8 W, $v = 20\ \text{mm/s}$, $f = 1\ \text{MHz}$

Beside the cracks that can occur along the laser beam axis due to the internal pressure in brittle glass material, other types of cracks have been observed which are shown in fig. 4 and 5. Along with the tunnel-like cracks (fig. 4) that extend around the molten zone another type of cracks runs perpendicular to the welding direction (fig. 5). Formation of the tunnel-like as well as the transverse cracks has been observed in all types of the tested glass but fused silica. The crack formation was most prominent for processing conditions where a high average power or low feed rate has been used. Since fused silica glass has more than an order of magnitude smaller thermal expansion coefficient ($0.5 \times 10^{-6}\ 1/\text{K}$ fused silica glass vs. $7.2 \times 10^{-6}\ 1/\text{K}$ for D263 glass [13,14]) we attributed the formation of these defects to the thermal expansion and shrinkage of the glass material and to the corresponding thermal expansion and shrinkage stresses.

The majority of industrial glasses have a thermal expansion coefficient that either lies in the same range as that of D263 or is even larger. In order to be able to weld these glasses with acceptable quality, the described cracking problem must be overcome. We expect that highly symmetrical molten zones and welding seams (achievable by focusing lenses with very high numerical apertures) will be less prone to the defects described in this section because rounded shapes distribute the thermally induced mechanical stress that originates from the center of the

molten zone more evenly. As has been shown in [8] defect free welding is possible when the processing parameters such as laser power, repetition rate, feed rate, and focusing geometry are chosen in the right way.

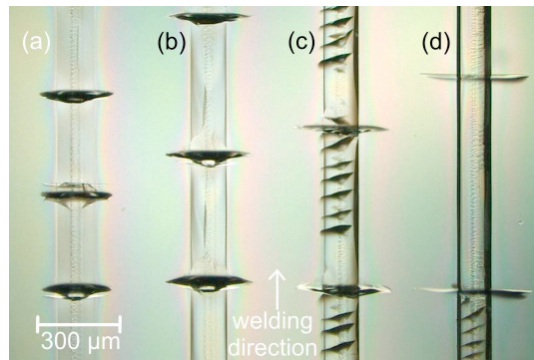


Fig. 5. Top view on the welding seams in D263 glass. Cracks perpendicular to the welding direction are clearly visible. In (b)-(d) also tunnel-like cracks can be observed. The welding conditions are: (a): NA = 0.55, P = 4 W, v = 20 mm/s, f = 700 kHz; (b): NA = 0.55, P = 4 W, v = 20 mm/s, f = 1 MHz; (c): NA = 0.55, P = 4 W, v = 20 mm/s, f = 2 MHz; (d): NA = 0.55, P = 4 W, v = 20 mm/s, f = 3.9 MHz

The ultrafast laser glass welding requires tight laser beam focusing to achieve electric fields sufficient for material ionization. Typically, the laser intensity is sufficiently high only within a quite small volume. For a typical laser beam size of 2 mm focused with NA = 0.8 objective lens the corresponding Rayleigh length is only 15 μm and the beam waist is $\sim 2 \mu\text{m}$, while the initial plasma volume can be even smaller. Consequently, in order to heat a glass joining interface efficiently the laser beam focus has to be positioned very precisely. Fig. 6 shows a cross-section of a welded sample, where the distance between the focal spot and the joining interface has been varied in steps of 10 μm . The cross section is observed under crossed polarizers in order to show regions with stress induced birefringence, which reflects a profile of the mechanical stress within the sample volume.

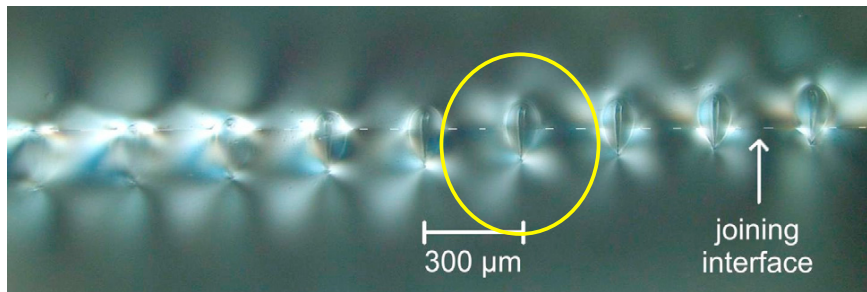


Fig. 6. Cross sections of two welded D263 glass plates observed under crossed polarizers. The focus displacement perpendicular to the joining interface is set in steps of 10 μm . Each welding seam was carried out under the same welding conditions: NA = 0.55, P = 6 W, v = 20 mm/s, f = 1 MHz. Laser beam propagation direction is indicated by the red arrow

As can be seen, the largest stress induced birefringence occurs when the upper or lower tip of the molten zone approaches the joining interface. By contrast, the stress induced birefringence, as well as the mechanical stress, is smallest when the thickest part of the molten zone is aligned with the joining interface as indicated by the yellow circle in fig. 6. This normally requires the laser beam to be focused slightly below the joining surface. Also, it should be pointed out that an incorrect positioning of the laser beam focus leads to the formation of cracks inside the welding seam and to the deformation of the joining surface as it can be seen in fig. 4 (a) and 7.

While the origin of the dependence of the welding seam shape and quality on the laser beam position is not completely understood it can be probably attributed to the nonuniform heating in the welding process. The material of the lower glass plate lies presumably in between the glass transition temperature and the melting point. Thus, the

material can be deformed, but the still considerable surface tension prevents a joining of the glass plates. However, the surface tension reduces with increasing temperature due to the Eötvös rule, so that proper heating of the lower joining partner should overcome this obstacle resulting in fully molten welding seams as shown in fig. 8. Further research work will be necessary to understand this phenomenon as well as to develop reliable laser beam positioning methods.



Fig. 7. Cross section of a welding seam in D263 under the following conditions $NA = 0.55$, $P = 6$ W, $v = 30$ mm/s, $f = 1$ MHz

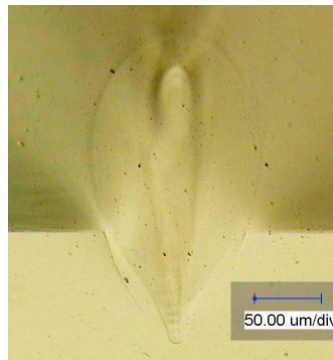


Fig. 8. Sample images of the weld seam obtained with optical microscope [8]. The sample is made of D263 glass. The feed speed is 20 mm/sec at 1 MHz repetition rate and an NA 0.55 objective is used. The laser power is 5 W

As has been shown in previous paragraphs the development of cracks is most probable if the material is comparably cold and thus brittle. Generally, the welding conditions can be chosen such that this problem is minimized during welding. However, at the beginning of the welding a situation is present when the laser hits cold and brittle material. The typical defects formed at the beginning of a welding seam are clearly visible in fig. 8.

One possible method to resolve this issue would be to reverse the direction of the welding and to melt up the cracked material. However, this would require, that the laser stops during the welding, which could cause the material to crack at the stopping position. Therefore, instead of changing the welding direction a circular welding seam could be used to effectively fuse the cracks at the starting point. The second possibility would be to ramp up the average power and the feed rate of the laser in such a way that the molten zone is allowed to grow slowly. The heating and thus the ductility of the material could keep pace with the induced mechanical stresses resulting in a reduced cracking tendency.

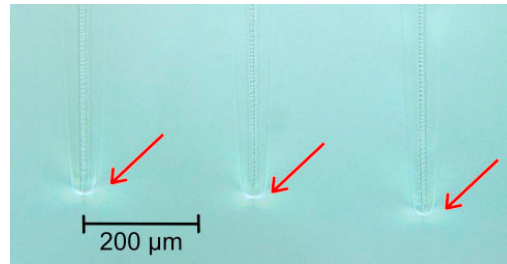


Fig. 9. Top view of cracks formed at the beginning of the welding seam in D263 under the following conditions $NA = 0.55$, $P = 6$ W, $v = 20$ mm/s, $f = 1$ MHz

4. Conclusion

The formation of defects and cracks can be categorized into two groups. The first group consists of cracks generated when the material is too cold and therefore brittle. The observed defects belonging to this category are longitudinal cracks (fig. 2), the incorrect positioning of the welding seam (fig. 7) and cracks at the beginning of the welding seam (fig. 8). The second group consists of cracks shown in fig. 4 and 5 where the volume of the molten zone grows so large that the thermal expansion and contraction lead to crack formation. As fused silica has a very low thermal expansion coefficient these types of defects were not observed in this material.

It has been shown that by using focusing objectives with a very high numerical aperture the formation of longitudinal cracks can be suppressed. It is to be expected that if a more uniform temperature distribution is established by using high numerical aperture objectives, the occurrence of defects in both defect categories can be reduced. However, when using objectives with high numerical apertures spherical aberrations induced by deep focusing must be taken into account.

References

- [1]: Naumann, H.; Schröder, G.: Bauelemente der Optik. Hanser Verlag München, 1992.
- [2]: H. Banse, Laserstrahllöten – Technologie zum Aufbau optischer Systeme, Dissertation, University Jena, 2005.
- [3]: V. Greco, F. Marchesini, G. Molesini: Optical contact and van der Waals interactions: the role of the surface topography in determining the bonding strength of thick glass plates, *J. Opt. A: Pure Appl. Opt.*, Vol. 3, pp 85-88, (2001).
- [4]: Grünwald, F.: Fertigungsverfahren in der Gerätetechnik. Carl Hanser Verlag München Wien, 1985.
- [5]: S. Hecht-Mijic, A. Harnisch, D. Hülsenberg, S. Schundau, J. Pfeifer, T. Schroeter, Thermisches Bonden von Bauteilen aus mikrostrukturiertem Glas, *Mat.-wiss. u. Werkstofftech.* 34, pp. 645–647, (2003).
- [6]: Y. Arata, H. Maruo, I. Miyamoto and S. Takeuchi, Dynamic Behavior of Laser Welding and Cutting, *Proc. of 7th International Conf. on Electron and Ion Beam Science and Technology*, New Jersey (1976), pp. 111 – 128.
- [7]: H. Maruo, I. Miyamoto and Y. Arata: “CO₂ Laser Welding of Ceramics”, *Proc. of 1st International Laser Processing Conference*, Anaheim, California November, 1981 [103] ms-pulses Nd:YAG glass welding.
- [8]: B. C. Stuart, M. D. Feit, S. Herman, A. M. Rubenchik, B. W. Shore, M. D. Perry: “Nanosecond-to-femtosecond laser-induced breakdown in dielectrics”, *Phys. Rev. B*, Vol. 54, No. 4, pp. 1749 – 1761, Jan. 1996
- [9]: A. S. Sandhu, A. K. Dharmadhikari, G. R. Kumar: “Time resolved evolution of structural, electrical, and thermal properties of copper irradiated by an intense ultrashort laser pulse”, *J. Appl. Phys.* 97, 023526 (2004)
- [10]: I. Alexeev, K. Cvecek, I. Miyamoto, M. Schmidt: “Ultrafast Laser Processing of Transparent Media – Glass Welding”, in *Proc. LEF 2010, Laser in der Elektronikproduktion & Feinwerktechnik*, Fürth, 2.-3. March, LEF Tagungsband 2010, Hrsg. M. Geiger, M. Schmidt, C. Kägeler, Meisenbach Bamberg 2010, pp. 125–137.
- [11]: I. Miyamoto, K. Cvecek, Y. Okamoto, P. Bechtold, M. Schmidt: “Laser-matter interaction in fusion welding of fused silica using ultrashort pulse lasers”, in *Proc. LAMP 2009, 5th International Congress on Laser Advanced Materials Processing*, Kobe 2009, 29 Jun. - 2 Jul., paper TuOL1.
- [12]: J. B. Pawley: “Handbook of Biological Confocal Microscopy”, 3rd ed., 2006, Springer.
- [13]: http://www.schott.com/lithotec/english/download/fused_silica_standard_grade_opto_jan_2010.pdf
- [14]: http://www.schott.com/special_applications/english/products/thin_glass/d263t.html#thermal